Electrochimica Acta 290 (2018) 165–175

Contents lists available at ScienceDirect

Electrochimica Acta

journal homepage: www.elsevier.com/locate/electacta

# Synergistic effects of electricity and biofilm on Rhodamine B (RhB) degradation in three-dimensional biofilm electrode reactors (3D-BERs)

Lei Feng [a, 1], Xiu-yan Li [a, 1], Li-hong Gan [a], Juan Xu [a, b, *]

[a] Shanghai Key Lab for Urban Ecological Processes and Eco-Restoration, School of Ecological and Environmental Sciences, East China Normal University, Shanghai, China
[b] Institute of Eco-Chongming, East China Normal University, Shanghai, China

ARTICLE INFO

*Article history:*
Received 28 July 2018
Received in revised form
10 September 2018
Accepted 11 September 2018
Available online 11 September 2018

*Keywords:*
Biofilm
Electro-biodegradation
Particle electrode
Rhodamine B (RhB)
Three-dimensional biofilm electrode reactors (3D-BERs)

ABSTRACT

Three-dimensional biofilm electrode reactors (3D-BERs) represent an environmentally acceptable and cost effective technology for refractory wastewater treatment. Previous studies on 3D-BERs primarily focused on treatment performance, and little information is available about the microscopic mechanisms of contaminant degradation. The reactions occurred on particle electrodes, the core units of the 3D-BERs served as both electrodes and biofilm carriers, are still unclear. This study comprehensively elucidated the synergistic effects of electricity and biofilm on Rhodamine B (RhB) removal in 3D-BERs from both macroscopic and microcosmic aspects. Continuous-flow 3D-BERs were operated to evaluate overall treatment performance. Batch experiments were conducted to explore the kinetics of RhB degradation as well as the contributions of various physical, chemical, and biological processes to RhB removal. The biofilm formed on the particle electrodes was characterized by imaging and microbial analyses. The results indicated that applying voltage promoted degradation of RhB. Three processes, including electro-adsorption, electrochemical oxidation and electro-biodegradation, were identified to contribute to RhB degradation. Microorganisms in the *Rhodanobacter* and *Thiomonas* genera were distinctively enriched under acclimation voltage, which was attributed to the accumulation of intermediates generated by electrochemical oxidation. This study demonstrated that the synergistic effects of electricity and biofilm were dependent on applying voltage, that would be beneficial to comprehensively understand the contaminants removal process in 3D-BERs.



## 1. Introduction

Dyeing wastewater causes serious environmental problems due to inherent chromaticity and toxicity. Rhodamine B (RhB) is one of the most important xanthene dyes widely applied in the textile industry to dye silk, wool, jute leather, and cotton [1]. RhB contamination threatens public health, as it irritates the skin, eyes and respiratory tract, and even be carcinogenic [2]. Various physical, chemical and biological techniques, such as adsorption, photocatalysis and enzymatic oxidation by white-rot fungi have been adopted to treat RhB wastewater [3]. However, satisfactory treatment performance was not achieved, as these techniques are either too expensive or inefficient.

Recently, bio-electrochemical technique has attracted increasing attention as an environmentally acceptable and cost effective method [4,5]. In particular, three-dimensional biofilm electrode reactors (3D-BERs) represent a novel technology for refractory wastewater treatment [6]. For example, 3D-BERs demonstrate excellent treatment performance in antibiotics wastewater containing sulfamethoxazole and tetracycline [7]. The 3D-BERs are also suitable for remediating nitrate in groundwater due to co-existing autotrophic and heterotrophic denitrification [8].

3D-BERs actually integrate biofilm and electrochemical technology, and take advantages from both treatment processes. In 3D-BERs, particles [e.g., granular activated carbon (GAC), zeolite, sulfur and iron] are filled between anode and cathode, not only serving as

* Corresponding author. Shanghai Key Lab for Urban Ecological Processes and Eco-Restoration, School of Ecological and Environmental Sciences, East China Normal University, Shanghai, China.
*E-mail address:* jxu@des.ecnu.edu.cn (J. Xu).
[1] Lei Feng and Xiu-yan Li contributed equal to this study.

https://doi.org/10.1016/j.electacta.2018.09.068
0013-4686/

the third bipolar electrode but also providing high surface area for biomass growth and attachment [9]. The immobilized biomass in the biofilm show more stable performances in refractory contaminants removal compared to the suspended biomass due to the higher biodegradation activity and tolerance to refractory contaminants [10]. Applying electricity influences the growth and metabolic behaviors of the microorganisms in the biofilm. It was reported that hydrogen and oxygen generated from electrolysis of water enhance cell growth and dehydrogenase activity, thus promoting degradation of contaminants [11]. In addition, electricity also accelerates cell death during the later stationary phase due to the presence of anodic intermediates including $H_2O_2$, OH• and $O_2$•, which facilitates reformation of the biofilm [11]. For example, phenol removal efficiency increased by 33% when an electric current (1.98 mA; 21 h) was applied to biofilm attached on propylene [12]. Electric current (0.42 mA/cm$^2$; 24 h) inhibits the growth of *Aspergillus niger* on perlite carrier, while increasing hexadecane biodegradation by 15% [13].

However, previous studies primarily focused on treatment efficiency of the contaminants, and little information is available about the microscopic mechanism of contaminants removal in 3D-BERs. In particular, as the core unit of the 3D-BERs, the particle electrodes with porous structure have strong adsorption capacity for contaminants. After being polarized by an external electrical field, physical, chemical, biological processes and their interactions occur simultaneously on the particle electrodes, which would significantly influence the overall treatment performance of the 3D-BERs. To date, little effort has been devoted to identify the specific contribution of adsorption, electricity and the biofilm formed on particle electrodes to contaminant removal.

Therefore, the aims of this study were: (1) to evaluate the performance of 3D-BERs in degrading RhB dyeing wastewater, which is a typical refractory contaminant containing carbon and nitrogen; (2) to characterize the particle electrodes in the 3D-BERs during the treatment process; and (3) to explore the synergistic effects of applying voltage and the biofilm formed on particle electrodes on RhB degradation. The results will provide useful information about particle electrodes and help to further understand the contaminant removal process in 3D-BERs.

## 2. Materials and methods

### 2.1. Chemicals

The fluorescent dyes including 4′,6-diamidino-2-phenylindole (DAPI), Nile Red, fluorescein isothiocyanate (FITC) and Fluorescent Brightener 28 were purchased from Sigma-Aldrich (St. Louis, MO, USA). The other reagents were from Sinopharm Chemical Reagent Co., Ltd. (Shanghai, China).

### 2.2. 3D-BER configuration

A schematic diagram of the 3D-BER was shown in Fig. S1. The 3D-BER was a rectangular polypropylene tank (200 × 100 × 90 mm) with an effective working volume of 1.5 L. The Ti/$RuO_2$-$IrO_2$ electrode (100 × 90 × 2 mm) located in the middle of the tank was set as the anode, and two stainless steel plates with the same dimensions were placed on both sides of the tank as the cathodes (Shuerde Industrial Machinery Co., Suzhou, China). The anode was carved into a grill shape with effective area of 62 cm$^2$ to ensure mass transfer in the tank. The anode and two cathodes were positioned vertically and parallel to each other with an inter-electrode gap of 100 mm, and the particle electrodes were packed between the anode and cathode. The particle electrodes were a mixture of GAC (3–5 mm diameter with a specific area of 800–1000 m$^2$/g) and zeolite (5–8 mm diameter with a specific area of 500–600 m$^2$/g) at a volume ratio of 1:1. GAC was frequently employed as the particle electrodes owing to its features of conductivity, chemical stability and high surface area. The zeolite was mixed to improve current efficiency by reducing inter current loop. The electric field was supplied by a digital DC power (CE0036030S; Earthworm Electronics Co. Ltd, Shanghai, China). Air was purged into the reactor at a flow rate of 100 L/h through a microporous aeration bar at the bottom of the tank.

### 2.3. Biofilm acclimation

The start-up process of the 3D-BERs was divided into biofilm cultivation and biofilm acclimation stages [14]. The microorganisms were inoculated from the campus river. During the cultivation period, the biofilm was cultivated using glucose as the carbon source [15]. The medium contained (in mg/L): glucose 250, $NH_4Cl$ 50, $KH_2PO_4$ 10, $ZnSO_4·7H_2O$ 0.2, $MnCl_2·4H_2O$ 0.12, $FeCl_3$ 0.6, $CoCl_2·6H_2O$ 0.24, $H_3BO_3$ 0.15, $CuSO_4·5H_2O$ 0.03, KI 0.18, and $NaMoO_4·2H_2O$ 0.06. No external electrical field was applied. After two weeks, the brown biofilm was observed attaching on the particle electrodes. Then, the acclimation period began. Different voltages (0, 3, 6, and 9 V) were applied to the four 3D-BERs, and the carbon source was gradually changed from glucose to RhB. After acclimation for 20 days, RhB was used as the sole carbon source for microbial growth.

### 2.4. Operation of the 3D-BERs

After the acclimation period, the four 3D-BERs (R1, R2, R3 and R4) were operated continuously by applying different voltages (0, 3, 6, and 9 V). The reactors were fed with a synthetic wastewater containing (in mg/L): RhB 200, $NH_4Cl$ 60, $K_2HPO_4$ 17.4, $ZnSO_4·7H_2O$ 0.2, $MnCl_2·4H_2O$ 0.12, $FeCl_3$ 0.6, $CoCl_2·6H_2O$ 0.24, $H_3BO_3$ 0.15, $CuSO_4·5H_2O$ 0.03, KI 0.18, $NaMoO_4·2H_2O$ 0.06. The influent was dosed into the 3D-BERs continuously by a peristaltic pump (BT100-1L; Baoding Longer Precision Pump Co. Ltd, Baoding, China) at a flow rate of 1.20 mL/min, corresponding to a hydraulic residence time (HRT) of 12 h. The HRT was altered from 12 to 24 h by adjusting the flow rate on days 7 and 14 during operation.

### 2.5. Characterization of the biofilms attached on the particle electrodes

#### 2.5.1. Morphology characterization by imaging

The morphology of the biofilm attached on particle electrodes was characterized by scanning electron microscopy (SEM) and confocal laser scanning microscopy (CLSM). The procedures were described in Supplementary Data.

#### 2.5.2. Quantification of biomass

The particle electrodes were mixed thoroughly by stirring with a spoon before sampling. A certain quantity of the particle electrodes were taken from each reactor and separated as GAC and zeolite to release the microorganisms from the particle electrodes for subsequent enumeration by plate counts. About 5 g of wet particles were transferred into conical flasks, and 0.05 M PBS (15 mL) was added into the flasks. The microtip of a sonic dismembrator (IID; Scientz, Ningbo, China) was wiped with 70% ethanol and then placed in the flasks such that the tip was approximately 2 cm above the surface of the particles. The sonic dismembrator was operated for 2 min at 39 W, and then the flask was placed on a vortex mixer for 1 min. The supernatant was transferred to a fresh cylinder. This process was repeated five times, yielding a total volume of 75 mL.

The particles were retained, dried and weighed. Heterotrophic plate counts were conducted for the supernatant with R2A agar after a 4 day incubation at 33 °C. Finally, the amount of biomass was calculated by counting the number of colonies on the cell culture medium [16].

### 2.5.3. Microbial analysis

Six particle electrodes samples were collected from the 3D-BERs at the end of the operating time and respectively tagged as R1-G and R1-Z (collected from the GAC and zeolite of R1); R3-G and R3-Z (collected from the GAC and zeolite of R3); R4-G and R4-Z (collected from GAC and zeolite of R4). The DNA of these samples was extracted using the E.Z.N.A.® Water DNA Kit (Omega, Madison, WI, USA). The quality and the quantity of the DNA were examined by 0.8% agarose gel electrophoresis (DYY-6C, Liuhe, Beijing, China) and spectrophotometrically quantified with a UV spectrophotometer (NC 2000, Thermo Scientific, Waltham, MA, USA). 16S rRNA genes for high-throughput sequencing were amplified using primers with a barcode. The primers were 338F (5′-ACTCCTACGGGAGGCAGCA-3′) and 806R (5′-GGACTACHVGGGTWTCTAAT-3′) targeting the V4 region of the 16S rRNA gene. Sequencing was completed on the Illumina Miseq platform (Illumina, San Diego, CA, USA) in Shanghai Personal Biotechnology Co., Ltd. The resulting high quality sequences were processed to generate operational taxonomic units (OTUs) and allocated to the kingdom, phylum, class, order, family and genus levels using the Mothur program [17].

## 2.6. Batch experiments

Four batch experiments (R1′, R2′, R3′, and R4’) were conducted to evaluate the kinetics of RhB degradation in the 3D-BERs. The degradation rate constants for RhB, total organic carbon (TOC) and total nitrogen (TN) were obtained by fitting the batch experimental data using a pseudo-first-order kinetic model as follows:

$$\ln C_t = -kt + \ln C_0 \quad (1)$$

Where $C_t$ (mg/L) is the RhB, TOC or TN concentration at time t; $C_0$ (mg/L) is the RhB, TOC or TN concentration at the initial time; and $k$ is the pseudo-first-order rate constant ($h^{-1}$).

In addition, four other 3D-BERs (R5′, R6′, R7′ and R8′) were set to identify the contribution of physical, chemical and biological processes to RhB removal. The particle electrodes in R5′, R6′, R7′ and R8’ were pretreated with sodium azide (1.0 g/L) for 12 h to inhibit microbial activity. The experimental conditions were listed in Table 1. The RhB removal efficiency by adsorption ($R_{Adsorption}$), biodegradation ($R_{Biodegradation}$), electro-adsorption and electrochemical oxidation ($R_{Electro\text{-}adsorption\ and\ oxidation}$) and electro-biodegradation ($R_{Electro\text{-}biodegradation}$) was calculated as follows:

$$R_{Effluent,0V} = \frac{C_{R1'}}{C_0} \times 100\% \quad (2)$$

$$R_{Effluent,3V} = \frac{C_{R2'}}{C_0} \times 100\% \quad (3)$$

$$R_{Effluent,6V} = \frac{C_{R3'}}{C_0} \times 100\% \quad (4)$$

$$R_{Effluent,\ 9V} = \frac{C_{R4'}}{C_0} \times 100\% \quad (5)$$

$$R_{Adsorption} = \frac{C_0 - C_{R5'}}{C_0} \times 100\% \quad (6)$$

$$R_{Biodegradation} = \frac{C_{R5'} - C_{R1'}}{C_0} \times 100\% \quad (7)$$

$$R_{Electro-adsorption\ and\ oxidation,3V} = \frac{C_0 - C_{R6'}}{C_0} \times 100\% \quad (8)$$

$$R_{Electro-adsorption\ and\ oxidation,6V} = \frac{C_0 - C_{R7'}}{C_0} \times 100\% \quad (9)$$

$$R_{Electro-adsorption\ and\ oxidation,\ 9V} = \frac{C_0 - C_{R8'}}{C_0} \times 100\% \quad (10)$$

$$R_{Electro-biodegradation,3V} = \frac{C_{R6'} - C_{R2'}}{C_0} \times 100\% \quad (11)$$

$$R_{Electro-biodegradation,6V} = \frac{C_{R7'} - C_{R3'}}{C_0} \times 100\% \quad (12)$$

$$R_{Electro-biodegradation,9V} = \frac{C_{R8'} - C_{R4'}}{C_0} \times 100\% \quad (13)$$

Where $C_R$ is the RhB concentration in different reactors at the designated time.

## 2.7. Analytical methods

Liquid samples withdrawn from the reactors were filtered through 0.45 μm nitrocellulose membranes before analysis. The RhB concentration was measured by a UV−Vis spectrophotometer (UV-1600, Mapada Instruments Co., Ltd., Shanghai, China) at 552 nm. TOC and TN were measured with a multi N/C® 3100 analyzer (Analytik Jena, Germany). Specific oxygen uptake rate

**Table 1**
Batch experimental design.

| Reactor | Voltage (V) | $NaN_3$ (g/L) | Removal Routes | | | |
|---|---|---|---|---|---|---|
| | | | Adsorption | Biodegradation | Electro-adsorption and electrochemical oxidation | Electro-biodegradation |
| R1′ | 0 | 0 | + | + | - | - |
| R2′ | 3 | 0 | - | - | + | + |
| R3′ | 6 | 0 | - | - | + | + |
| R4′ | 9 | 0 | - | - | + | + |
| R5′ | 0 | 1 | + | - | - | - |
| R6′ | 3 | 1 | - | - | + | - |
| R7′ | 6 | 1 | - | - | + | - |
| R8′ | 9 | 1 | - | - | + | - |

+ effective removal route; - invalid removal route.

(SOUR) was determined according to the method described by Zheng [18].

The intermediates of RhB decomposition were analyzed on a gas chromatography-mass spectrometry (GC-MS) system (7890A-5975C; Agilent Technologies, Palo Alto, CA, USA). The pretreatment process was different for the intermediates on the particle electrodes and in the effluent. The 50 g particle electrodes were immersed in 50 mL $CH_2Cl_2$ and sonicated for 5 min, and this process was repeated three times. The supernatant was collected for further treatment. Intermediates in the effluent (25 mL) were extracted three times using 25 mL $CH_2Cl_2$. The liquid samples from the particle electrodes and effluent were dehydrated with anhydrous sodium sulfate and dried under a stream of nitrogen. The residue was dissolved in 1.0 mL of $CH_2Cl_2$ to identify the intermediates. Helium gas was used as the carrier in splitless mode, and a HP-5MS capillary column (30 m × 250 μm × 0.25 μm) was adopted. The temperature program followed an initial temperature of 50 °C held for 3 min, then ramped to 310 °C at 5 °C/min, and finally held at 310 °C for 25 min. Electron impact mode at 70 eV was selected for MS with an electron multiplier voltage of 1000 V. The intermediates were analyzed based on the NIST14 mass spectral library database [19].

## 3. Results

### 3.1. Effects of HRT and cultivating voltage on RhB removal in 3D-BERs

The removal of RhB in the four continuous-flow 3D-BERs under different cultivating voltages were displayed in Fig. 1a. Decolorization efficiency increased gradually with the extended HRT in the four 3D-BERs. Decolorization efficiency had no significant difference for R1, R2 and R3 when HRT was 12 h ($p = 0.093$). This was because a short HRT resulted in the accumulation of RhB on the particle electrodes and coverage of the reaction sites. The roles of electricity were not obvious under a lower voltage condition. The average decolorization efficiency for R4 with 9 V was 45.6%, which was clearly higher than those values for the other 3D-BERs. Decolorization efficiency was unstable during the HRT of 12 h. The decline in decolorization efficiency was also related to the short HRT, which induced temporary accumulation of RhB on the particle electrodes. Similar results were observed by Ailijiang et al. [20], who reported that phenol removal efficiency decreased significantly in conductive carriers supported biofilms of a bioelectrochemical reactor by shortening HRT from 14 to 10 h. Decolorization efficiency was similar in R1 and R2 when the HRT was 18 h. However, the average decolorization efficiency increased to 55.1% and 59.6% for R3 and R4, respectively. Discrepancies appeared for the four 3D-BERs after adjusting the HRT to 24 h, as the contribution of electricity became significant. However, decolorization efficiency of R2 was lower than that of R1, indicating that 3 V was outside the optimum range to improve RhB removal efficiency [21,22]. The average decolorization efficiency were 54.7%, 51.7%, 58.1% and 71.9% for R1, R2, R3 and R4, respectively.

The evolution of TOC removal efficiency in Fig. 1b was similar to that of decolorization efficiency. Removal efficiency of TOC increased with a prolonged HRT. Similarly, no significant difference in TOC removal was observed for the four 3D-BERs when HRT was 12 h ($p = 0.106$). R4 had a higher TOC removal efficiency under 18 h HRT, while the other three 3D-BERs had no obvious difference. R1 and R2 showed similar TOC removal performance when the HRT was 24 h ($p = 0.064$). The average TOC removal efficiency increased to 61.7% and 73.3% for R3 and R4, respectively.

Removal of TN in the 3D-BERs was displayed in Fig. 1c. The removal efficiency of TN decreased gradually with operation time

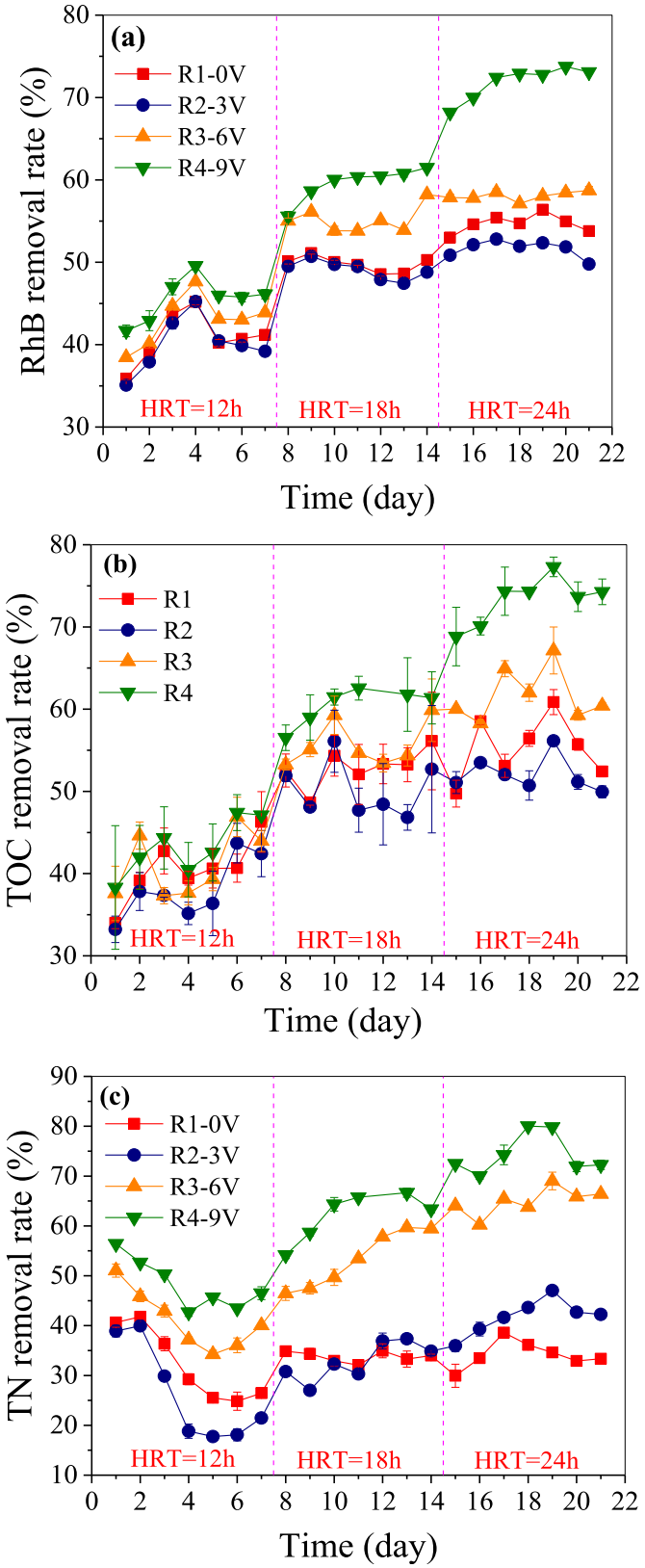


**Fig. 1.** Effect of HRT on (a) RhB decolorization efficiency; (b) TOC removal; (c) TN removal in 3D-BERs under different voltages.

in the four 3D-BERs when the HRT was 12 h. The average removal efficiency were 32.1%, 26.4%, 41.1% and 48.3% for R1, R2, R3 and R4, respectively. R1 and R2 maintained stable TN removal efficiency when the HRT was extended to 18 h. The TN removal efficiency increased from 46.5% to 59.5% in R3 and from 54.2% to 63.4% in R4. TN removal efficiency increased slightly in R2 with the longer HRT of 24 h, and exceeded that of R1. TN removal efficiency increased continuously in R3 and R4, with average values of 65.0% and 74.4%. TN removal was highly related to the electrochemical effect discussed in the following section.

### 3.2. Kinetics of RhB degradation in the 3D-BERs

The kinetics of RhB decolorization in the 3D-BERs were shown in Fig. 2. Rapid decolorization was observed during the first 0.5 h (Fig. 2a and b), owing to adsorption/electro-adsorption of the particle electrodes. As shown in Fig. 3, the decolorization rate increased gradually from 0.0294 $h^{-1}$ (0 V) to 0.0419 $h^{-1}$ (6 V) with increasing voltage. The rate constant increased dramatically to 0.1024 $h^{-1}$ when 9 V was applied, suggesting that the decolorization rate was improved by 3.5 times compared to the bioreactor

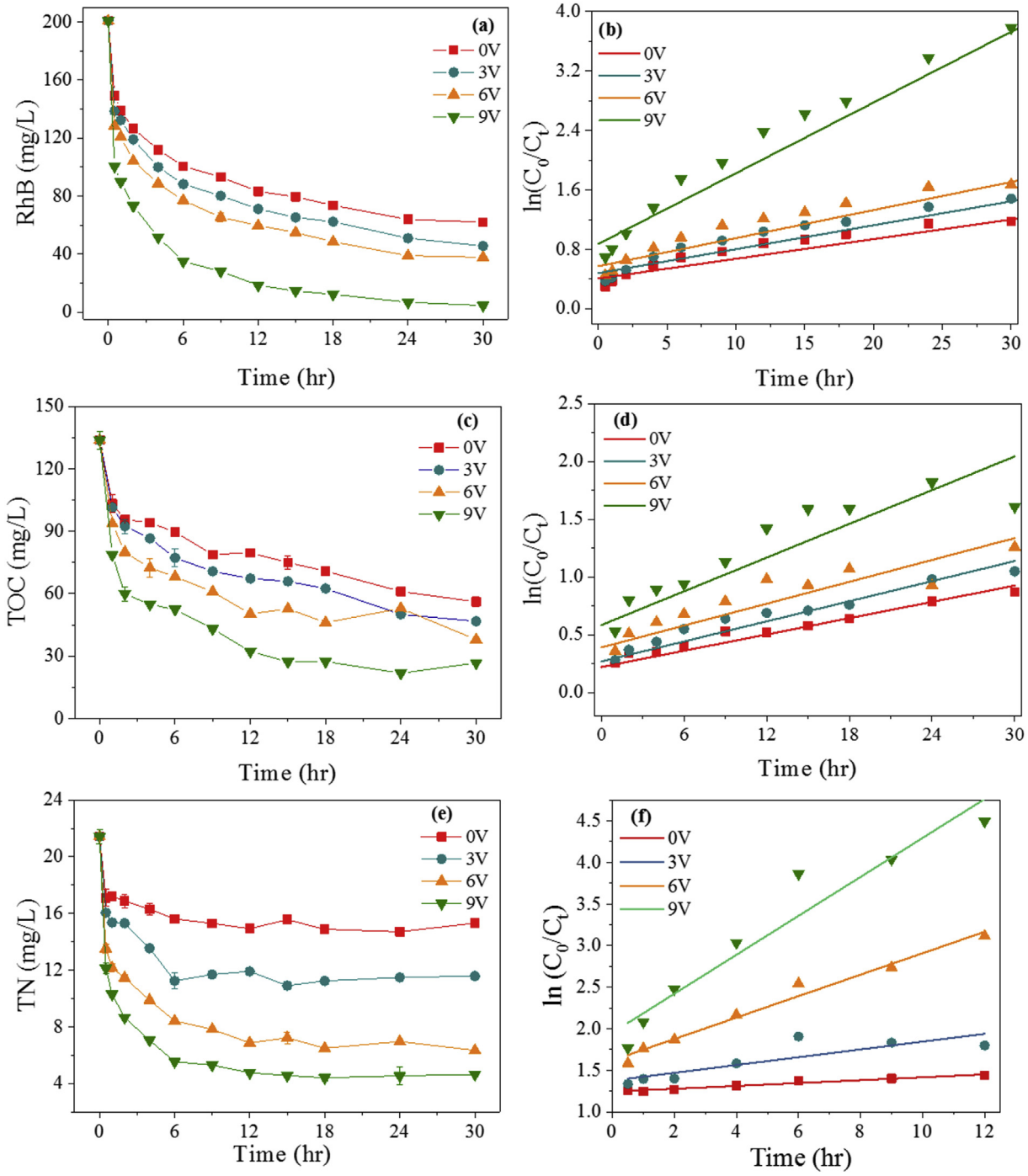


**Fig. 2.** Kinetics analysis of RhB degradation in 3D-BERs under different voltages: (a) evolution of RhB concentration; (b) first-order kinetic plot of decolorization; (c) evolution of TOC concentration; (d) first-order kinetic plot of TOC removal; (e) evolution of TN concentration; (f) first-order kinetic plot of TN removal.

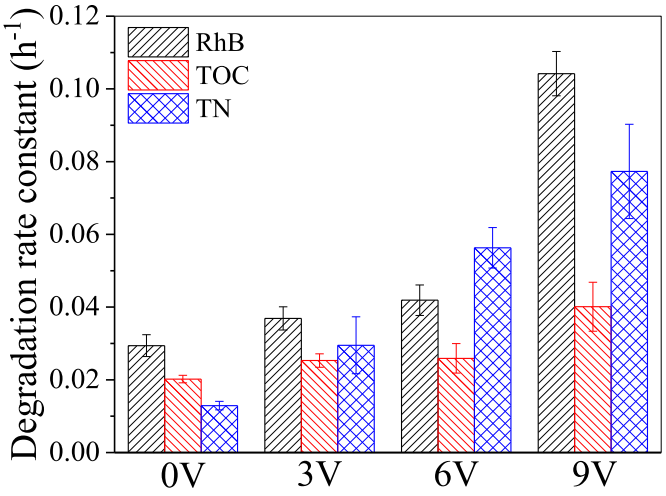


**Fig. 3.** Pseudo-first-order kinetics constants for the removal of RhB, TOC and TN under different voltages.

without voltage.

The kinetics of TOC degradation were shown in Fig. 2c and d. The rate constants were 0.0202, 0.0253, 0.0259 and 0.0401 $h^{-1}$ for 0, 3, 6 and 9 V (Fig. 3). The degradation of TOC was enhanced by gradually increasing the voltage. The 3 V and 6 V voltage led to a slight elevation in the TOC degradation rate, whereas 9 V promoted the degradation rate by two times compared to the bioreactor without voltage. The TOC degradation rate was slower than the RhB decolorization rate, revealing that mineralization was more difficult than decolorization for RhB removal.

Fig. 2e and f indicated the kinetics of TN removal in the 3D-BERs. Unlike RhB decolorization and TOC removal, degradation of TN was completed in 12 h due to the relatively low initial concentration. The degradation rate constants were 0.0129, 0.0295, 0.0562 and 0.0773 $h^{-1}$ respectively for 0, 3, 6 and 9 V (Fig. 3). Voltage had a clear significant positive effect on TN removal. A linear relationship existed between applied voltage and the TN degradation rate constant ($R^2 = 0.9928$), suggesting that TN removal was mainly due to the electrochemical effect.

### 3.3. Formation of biofilm on the particle electrodes

The morphology of the biofilm formed on the particle electrodes was characterized by SEM. GAC and zeolite were mixed together as the particle electrodes in this study, and both materials were covered by the biofilms (Fig. S2). There existed amounts of holes on the GAC and zeolite, providing adequate area for microbial growth. The coverage rate of the biofilm formed on GAC was higher than that on zeolite, which was attributed to the higher specific surface area of GAC. After acclimation with voltage, the biofilms remained attached on the GAC and zeolite, indicating that microbes with tolerance to electricity were enriched on the particle electrodes.

The distribution of biofilm on the particle electrodes was also characterized by CLSM. Four components of the biofilm, including nucleic acids, proteins, β-linked polysaccharides and lipids were labeled with fluorescent dyes. The biofilm on GAC displayed a dot-like distribution (Fig. 4), while the biofilm was distributed evenly on the surface of the zeolite (Fig. S3). The fluorescence intensity of the four components on the zeolite was stronger than that on GAC, suggesting a thicker biofilm formed on zeolite. Fig. 4 compared the fluorescence staining results of the biofilm on the GAC from R1 and R4. The fluorescence intensity of the GAC biofilm in R1 was stronger than that in R4, particularly for β-polysaccharides and lipids, indicating that high voltage generally inhibited the formation of biofilm on the GAC although some microbes survived.

The biomass on the GAC and zeolite were collected to quantify total microorganisms on the particle electrodes to evaluate the influence of electricity on microbial growth. Fig. 5a showed that the amount of biomass on the GAC was one to two orders of magnitude higher than that on zeolite, depending on the acclimation voltage. This was attributed to the larger specific surface area of GAC compared to zeolite, which was beneficial to the microbial

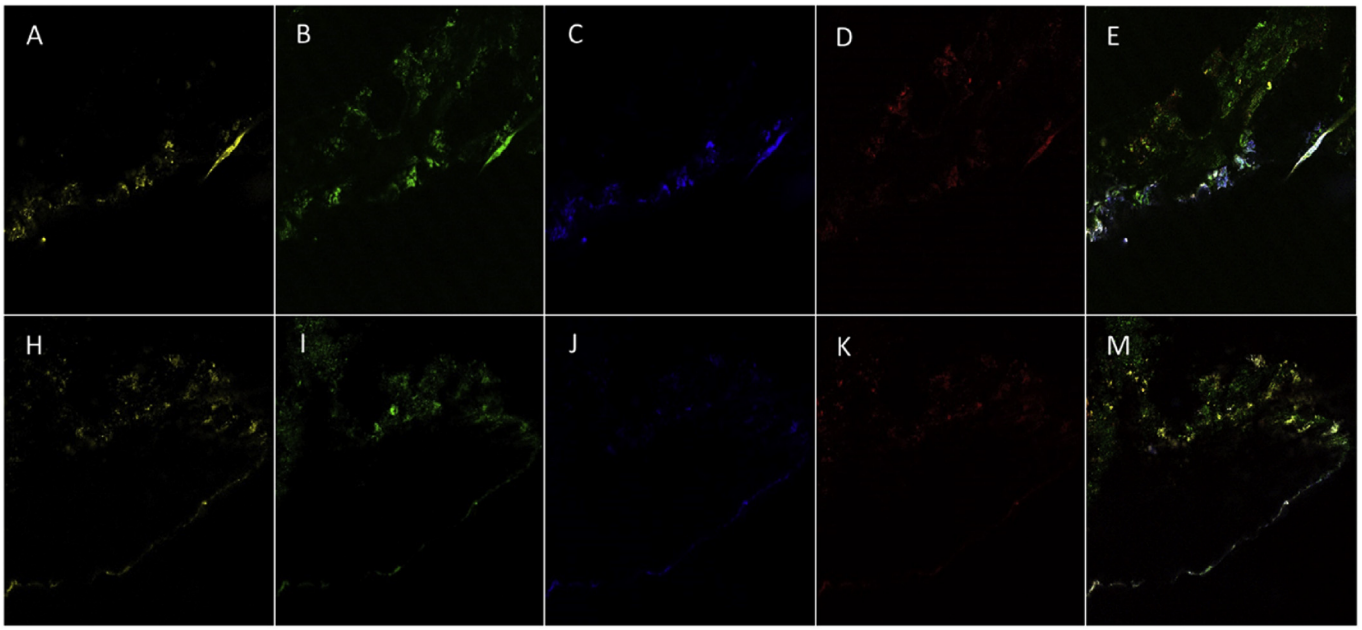


**Fig. 4.** The CLSM images of stained GAC in R1 (A–E) and R4 (H–M): A, H CLSM image of nucleic acids (DAPI). B, I CLSM image of proteins (FITC). C, J CLSM image of β-polysaccharides (FB28). D, K CLSM image of lipids (Nile red). E, M Combined image of individual images in A-D and H-M. (For interpretation of the references to color in this figure legend, the reader is referred to the Web version of this article.)

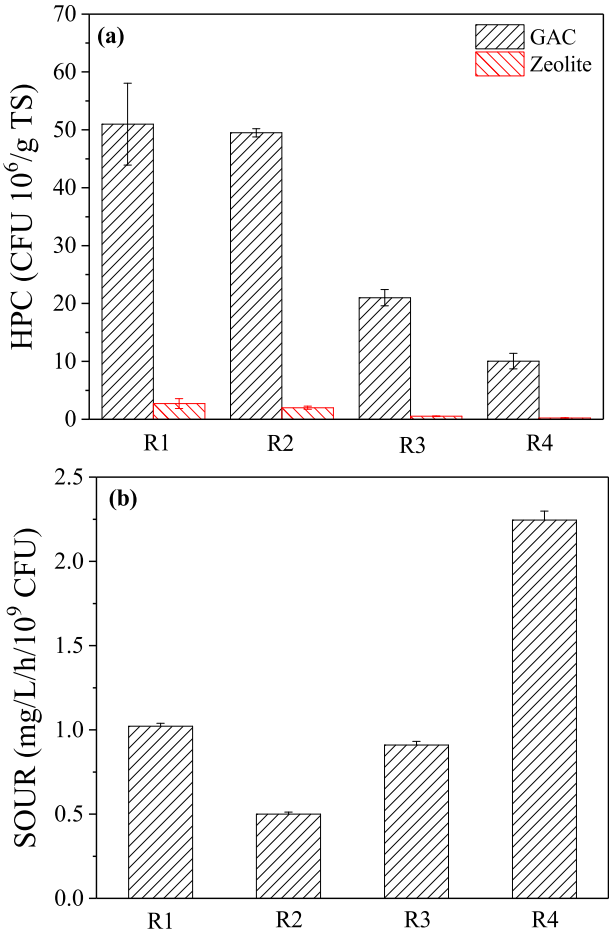


**Fig. 5.** (a) The number of microbes attached on the particle electrodes; CFU: colony-forming unit, HPC: heterotrophic plate count, TS: total solids; (b) SOUR of microbes attached on the particle electrodes.

adhesion. In addition, the degradation intermediates of RhB by electrochemical oxidation occurred on the polarized GAC particle electrodes could be utilized by microorganisms directly, accelerating microbial growth. The amount of biomass on the particle electrodes was similar for R1 without voltage and R2 with 3 V voltage (about 4 mA current). Ailijiang et al. also reported no significant difference in biomass of BERs with a 2 mA current and without current using conductive carbon felt as the biofilm carrier [20]. Microbial growth on the particle electrodes was inhibited significantly with a further increase in voltage. The decline in the biomass in response to current was mainly due to metabolic changes. Similar results were reported by other studies. Velasco-Alvarez et al. [13] demonstrated that applying an electric field (0.42 mA/cm$^2$) modified the metabolism of *A. niger*, reorienting it towards catabolism. The electric current reduced microbial growth by 52%, while hexadecane substrate degradation improved from 81% to 96%. They also found that when *A. niger* immobilized on perlite was pretreated with an electric current (0.42 mA/cm$^2$), its biodegradation activity for hexadecane was nine-fold higher than that of untreated biomass, but biomass production was only 20% [23]. Podolska et al. [24] showed that applying electric pulses (20 V) to *Pseudomonas fluorescens* could modify respiratory activity and the changes were reversible. Lustrato et al. [25] clarified that electric current (200 mA) improved the concentration of ATP in *S. cerevisiae*, due to changes in the electrochemical membrane potential which affect membrane transport and process energy transfer. In the present study, the R3 and R4 currents were measured as 18 mA and 45 mA, resulting in improved RhB degradation and reduced biomass production due to changes in metabolism.

### 3.4. Microbial community on particle electrodes in 3D-BERs

Illumina high-throughput sequencing of the 16S rRNA gene was employed to analyze the richness and diversity of the microbial communities on the particle electrodes in the 3D-BERs. The numbers of OTUs in the GAC and zeolite samples were much higher in R1 than those in R3 and R4, corresponding to the higher Shannon index, Chao1 values and abundance-based coverage estimator (ACE) values (Table 2). These results indicated that electric acclimation resulted in a remarkable reduction of species richness and diversity in the microbial communities on the particle electrodes, regardless of the material (GAC or zeolite). The richness of the microbial community on the particle electrodes in R4 (9 V acclimation) was slightly higher than that in R3 (6 V acclimation), but diversity was similar.

In addition, the number of OTUs, Chao1 and ACE values of R1-G (1071, 1160 and 1216) were higher than those of the R1-Z samples (998, 1073 and 1131). This finding indicated that microbial abundance and diversity of the biofilm on the GAC were higher than those on the zeolite, which was attributed to the higher specific surface area of the GAC for biofilm adhesion. Microbial abundance and diversity of the biofilm remained higher on the GAC than zeolite after R3 and R4 were acclimated to electricity. It was considered that the GAC could be polarized as microelectrodes, being able to transfer electrons directly to the biofilm. Thus, it was favorable for enriching the bacteria with bio-electrochemical function on GAC, resulting in more richness and diversity of bacteria on the GAC particle electrode.

Relative bacterial community abundance on the particle electrodes in the different 3D-BERs at the phylum level was shown in Fig. 6. *Proteobacteria* was the predominant phylum, with sequence percentages ranging from 46.7% to 95.1%. *Bacteroidetes*, *Firmicutes*, and *Acidobacteria* were the subdominant groups, comprising 0.3–29.3%, 0.1–8.2% and 0.6–5.0% of the taxa, respectively. The increase in voltage prompted the relative abundance of *Proteobacteria*, revealing that electricity stimulated the growth of *Proteobacteria*. In contrast, the relative abundance of *Bacteroidetes*, *Planctomycetes* and *Acidobacteria* decreased with increasing voltage, indicating that metabolism of those bacterial populations was inhibited by the high voltage. *Chloroflexi*, *Gemmatimonadetes*, *Chlorobi* almost disappeared under 9 V, indicating that the metabolism of those bacterial populations was significantly inhibited. These results verified that biofilm acclimated to electricity reflected remarkable differences in abundance and diversity of the bacterial community at the phylum level.

**Table 2**
Species diversity and abundance index of 6 samples from 3D-BERs.

| Sample | Chao1[a] | ACE[a] | Shannon[b] | OTUs[b] |
|---|---|---|---|---|
| R1-G | 1160 | 1216 | 7.57 | 1071 |
| R1-Z | 1073 | 1131 | 7.4 | 998 |
| R3-G | 528 | 528 | 5.15 | 528 |
| R3-Z | 491 | 491 | 4.91 | 491 |
| R4-G | 611 | 666 | 4.93 | 551 |
| R4-Z | 536 | 564 | 4.31 | 494 |

The R1-G and R1-Z, R3-G and R3-Z, R4-G and R4-Z represent biofilm samples from the GAC and zeolite of R1, R3 and R4 respectively.

[a] The abundance index of microbial community. A higher number represents more abundance.

[b] The diversity index. A higher number represents more diversity.

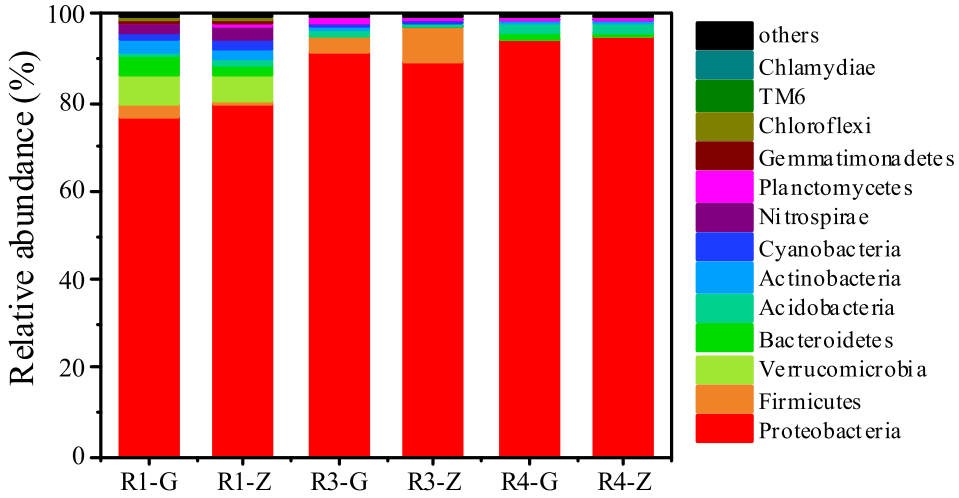


**Fig. 6.** Bacterial communities at phylum level (relative abundance over 0.1%).

*Rhodanobacter* and *Hyphomicrobium* were abundant genera in the three reactors (Fig. 7). The relative abundance of *Rhodanobacter* increased significantly in R3 with an acclimation voltage of 6 V. *Rhodanobacter* has demonstrated with capability to efficiently degrade a wide range of polycyclic aromatic hydrocarbons (PAHs) [26,27], which were typical intermediates of RhB generated by electrochemical degradation [28]. The enrichment of *Rhodanobacter* implied cooperation between electrochemical oxidation and biodegradation, exhibiting synergistic effects of electricity and the biofilm on RhB removal. The intermediate components changed with the higher acclimation voltage of 9 V in R4 (Table S1), causing *Rhodanobacter* to decrease and *Thiomonas* to increase. The relative abundance of *Thiomonas* in R4 was clearly higher than in the other bioreactors. *Thiomonas* had the competence of oxidizing sulfur, ferrous iron and arsenite [29] and exhibited heterotrophic growth with pyruvate [30]. These results indicated that the bacterial community at the genus level was related to the accumulated RhB degradation intermediates by electrochemical oxidation under the different acclimation voltages. In addition, applying voltage inhibited the relative abundance of *Ochrobactrum* and *Opitutus*, a

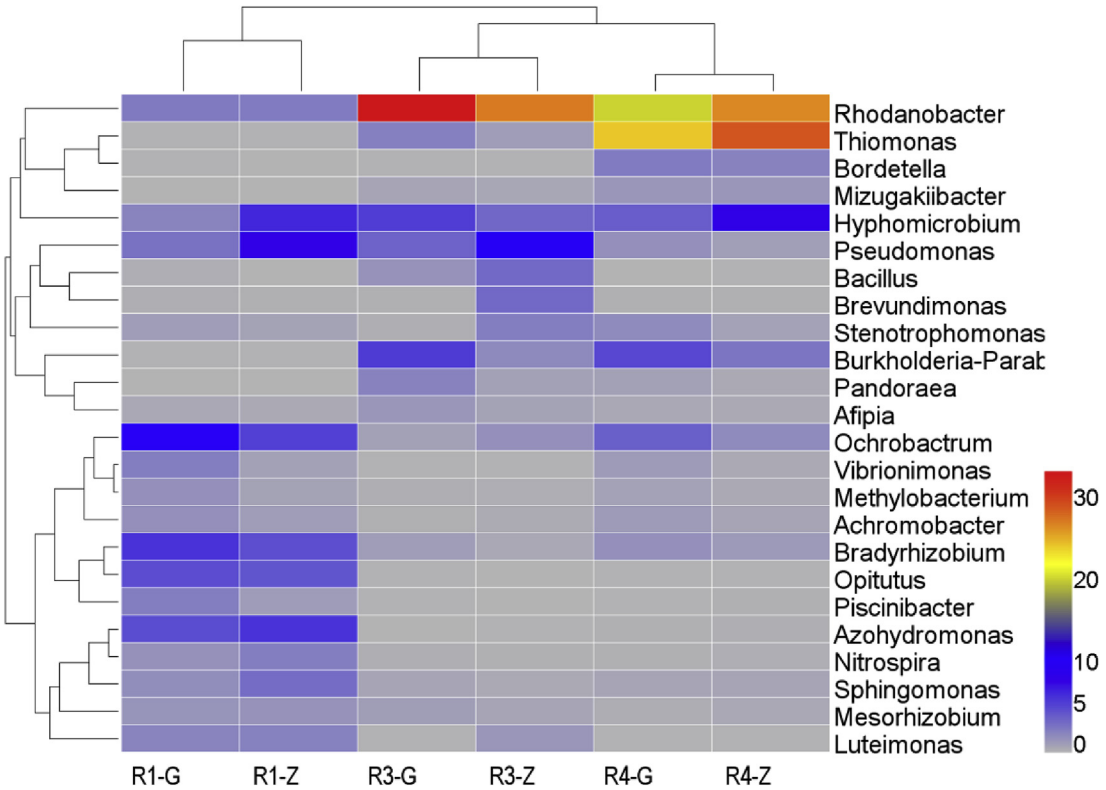


**Fig. 7.** Heat map of the most abundant genera in the 6 samples. Only the top 24 genera were used to build the heat map, and the color intensity shows the relative abundance of genus in the sample. (For interpretation of the references to color in this figure legend, the reader is referred to the Web version of this article.)

hydrogenotrophic denitrifying bacteria [31] and anaerobic fermentation bacteria [32]. These sensitive genera were mainly from the phylum *Proteobacteria*.

## 4. Discussion

### 4.1. Contributions of different removal routes to RhB degradation in the 3D-BERs

There were several mechanisms for RhB removal in the 3D-BERs, including adsorption, biodegradation, electro-adsorption, electrochemical oxidation and electro-biodegradation, which reflected the synergistic effects of electricity and biofilm on RhB removal. The contribution of the different removal routes to RhB degradation was in dependent on the voltage applied (Fig. 8).

Adsorption and biodegradation determined the RhB removal process in the 3D-BER without external voltage (Fig. 8a). The particle electrodes and the adhered biofilm comprised a very complex system, which had an excellent adsorption capacity for RhB molecules. The biofilm utilized RhB enriched on the particle electrodes as carbon source for biodegradation.

After applying voltage, the contribution of electro-adsorption and electrochemical oxidation appeared as shown in Fig. 8b–d. When an external electrostatic field was applied, two sides of the particle electrodes gathered positive and negative charges, respectively. These charged ions shifted to the opposite side of the charged particle electrodes, resulting in electro-adsorption [33]. Each particle electrode was like a micro-electrolytic cell when the polarized microelectrodes formed. Direct electro-oxidation on the polarized particle electrodes and indirect electro-oxidation with *in situ* generation of strong oxidants (e.g., $H_2O_2$, $Cl_2$ and HClO) decomposed contaminants quickly [33]. The combination of electro-adsorption and electrochemical oxidation ensured continuous regeneration of the particle electrodes, sustaining the stable operation of the 3D-BERs. Fig. 8e displayed the contribution of electro-adsorption and oxidation to RhB removal under different voltages. The roles of electricity were significant under the condition of applying 9 V voltage, with the contribution being more than 95%.

Electro-biodegradation is another mechanism for RhB removal in the 3D-BERs, resulting from the synergistic effects of the biofilm and the applied voltage. As shown in Fig. 8f, the contribution of electro-biodegradation increased first and then declined. This might be related to the substrate concentration accumulated on the particle electrodes. The RhB enriched on the particle electrodes increased gradually at the initial stage, which was favored by the microbes in the biofilm, and utilized as substrates for metabolism. Microbial activity was high, leading to increasing contribution of biodegradation. Excessive amounts of RhB accumulated on the particle electrodes with the extended reaction time, which in turn, inhibited microbial activity. Baldev et al. reported that 100 mg/L of RhB dye was optimum for effective decolorization by microalgae, while a higher concentration remarkably inhibited degradation efficiency [1]. Electro-biodegradation was influenced remarkably by the voltage applied. The optimum voltage of 6 V enhanced biodegradation effectively compared to the reactor without voltage. However, 3 V and 9 V weakened the contribution of biodegradation to RhB removal. This results was consistent with Li et al. [12], who demonstrated that the optimum electric field increased phenol biodegradation.

The treatment efficiency of the 3D-BERs for RhB was determined by combining the contributions of adsorption, electrochemical degradation and electro-biodegradation. For example, after treating for 6 h, RhB removal efficiency was 49.7% in R1′ without voltage. The particle electrodes and the biofilm absorbed 19.6% of the RhB while the biofilm degraded 30.1% of the RhB. At the same time, RhB removal efficiency increased to 61.5% in R3′ when 6 V was applied. Electro-adsorption and electrochemical oxidation were responsible for 28.0% of the RhB removal. Electro-biodegradation, denoted as the synergistic effect of electricity and biofilm, removed 33.5% of the RhB. The contributions of electro-adsorption and electrochemical oxidation, and electro-biodegradation were 63.7% and 18.8% when 9 V was applied in R4', which led to a removal efficiency of 82.5%. Thus, applying voltage accelerated the RhB removal process. Synergistic effects of electricity and biofilm appeared under the 6 V condition in this study.

### 4.2. Synergistic effects of electricity and biofilm on RhB removal under 6 V voltage

The positive roles of 6 V voltage in promoting the biodegradation of RhB may be caused by possible reasons as follows:

(1) By current stimulation, the cell membrane expanded so that nutrients could easily pass through the cell membrane to promote growth of the microorganisms [11]. In this study, the amount of biomass on the particle electrodes decreased significantly in response to 6 V voltage (Fig. 5a). Hence, the amount of biomass was not the predominant factor influencing RhB biodegradation.

(2) Under the electric field, the activity of specific enzymes in the microbes could be enhanced to accelerate the biological reaction [23]. SOUR could indicate the biological activity of the microorganisms (Fig. 5b). SOUR for microbes in R3 under 6 V were lower than the control group without voltage. It was noticed that the SOUR was determined in the absence of electricity, so it only represented microbial activity without stimulation by electricity. Similar results were observed in other studies [22], in which removal efficiency of the bioreactors was not only dependent on the SOUR values. Thus, neither did the microbial activity dominant RhB biodegradation.

(3) Refractory substances was converted to bioavailable intermediates by electrochemical oxidation, which could be directly utilized by microbes as carbon source for further removal [34]. The microbial analysis of the particle electrodes indicated that electric acclimation enriched some functional microbes. The abundance of *Rhodanobacter* increased significantly after applying 6 V but decreased with a further increase to 9 V. *Rhodanobacter* was a bacterial consortium that rapidly degraded a wide range of PAHs. Based on the GC-MS results in Table S1, PAHs, i.e., phenanthrene, were typical intermediates detected in R3 after applying 6 V while they were absent in R1 without voltage. The enrichment of *Rhodanobacter* implied the accumulation of RhB intermediates by electrochemical oxidation under the 6 V condition. The RhB intermediates changed with the increase in applied voltage to 9 V, resulting in a decrease of *Rhodanobacter*. These results reflected the cooperation of electricity and biofilm to RhB removal under the 6 V condition. The intermediates generated by electrochemical oxidation were further removed by electro-biodegradation, providing a new degradation pathway for removing RhB. This might be the main reason for promoted biodegradation of RhB in the 3D-BERs under the 6 V voltage. A synergy of electricity and biofilm was achieved by adjusting the voltage appropriately.

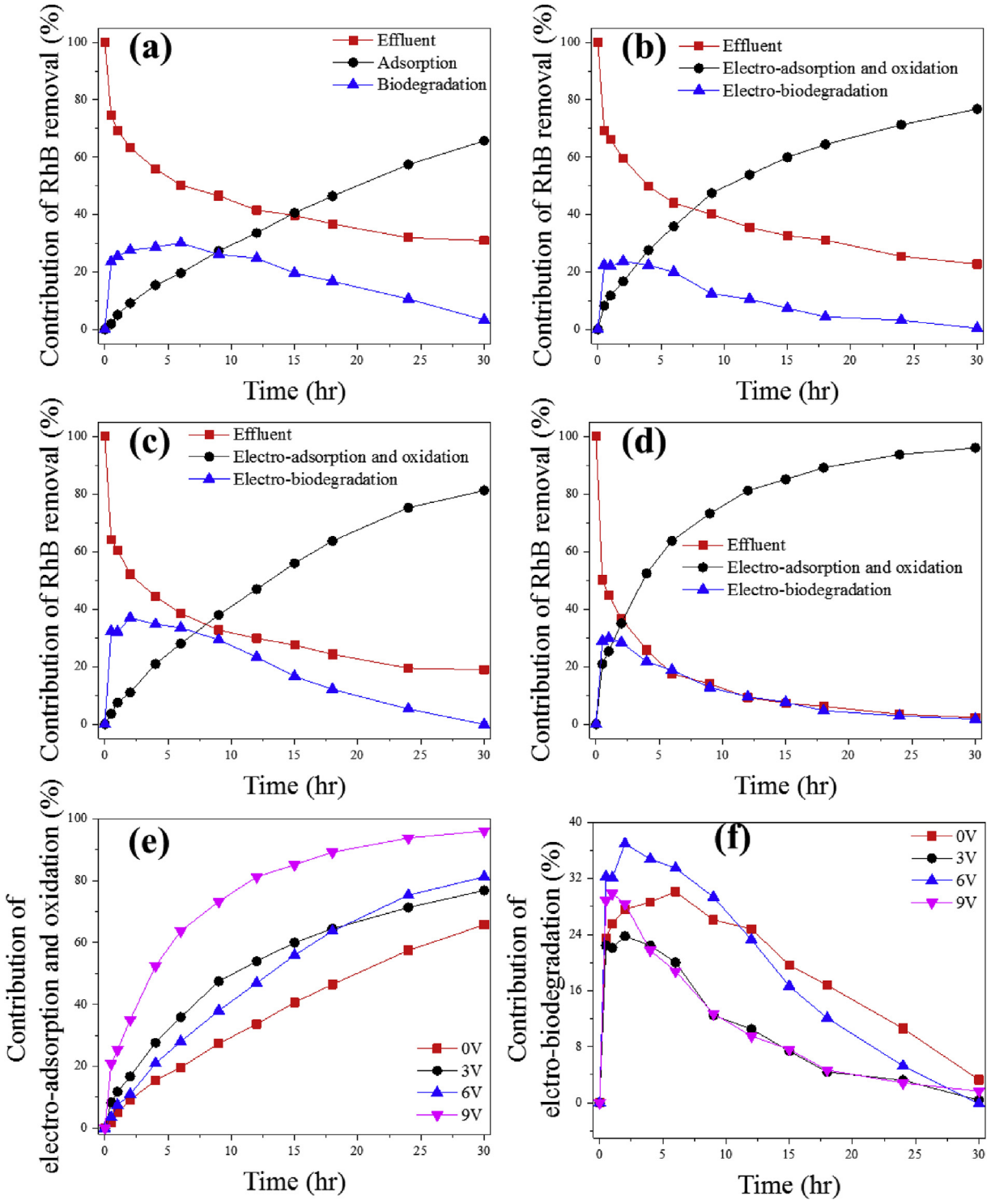


**Fig. 8.** The contribution of adsorption, biodegradation, electro-adsorption and oxidation, and electro-biodegradation to RhB removal under the voltage of (a) 0 V, (b) 3 V, (c) 6 V and (d) 9 V; The contribution of electro-adsorption and electrochemical oxidation (e) and electro-biodegradation (f) to RhB removal under different voltages.

## 5. Conclusions

Applying voltage promoted the degradation of RhB in the 3D-BERs. Specific microorganisms in the *Rhodanobacter* and *Thiomonas* genera were distinctively enriched despite inhibition of microbial growth on the particle electrodes. The intermediates generated by electrochemical oxidation were utilized by the microbes in the biofilm for further RhB removal, denoting as electro-biodegradation. Electro-adsorption, electrochemical oxidation and electro-biodegradation contributed differently to RhB removal, depending on the applied voltage. This study elucidated the synergistic effects of electricity and biofilm on contaminant removal and identified important roles of electro-biodegradation process.

## Acknowledgements

The authors wish to thank National Natural Science Foundation of China (51708224) for the support of this study.

## Appendix A. Supplementary data

Supplementary data to this article can be found online at https://doi.org/10.1016/j.electacta.2018.09.068.

## References

[1] E. Baldev, D. MubarakAli, A. Ilavarasi, D. Pandiaraj, K.A.S.S. Ishack, N. Thajuddin, Degradation of synthetic dye, Rhodamine B to environmentally non-toxic products using microalgae, Colloids Surfaces B Biointerfaces 105 (2013) 207–214.
[2] R. Jain, M. Mathur, S. Sikarwar, A. Mittal, Removal of the hazardous dye rhodamine B through photocatalytic and adsorption treatments, J. Environ. Manag. 85 (2007) 956–964.
[3] J. Ji, Y. Liu, X.Y. Yang, J. Xu, X.Y. Li, Multiple response optimization for high efficiency energy saving treatment of rhodamine B wastewater in a three-dimensional electrochemical reactor, J. Environ. Manag. 218 (2018) 300–308.
[4] R.A. Rozendal, H.V.M. Hamelers, K. Rabaey, J. Keller, C.J.N. Buisman, Towards practical implementation of bioelectrochemical wastewater treatment, Trends Biotechnol. 26 (2008) 450–459.
[5] N. Xafenias, Y. Zhang, C.J. Banks, Enhanced performance of hexavalent chromium reducing cathodes in the presence of shewanella oneidensis MR-1 and lactate, Environ. Sci. Technol. 47 (2013) 4512–4520.
[6] R. Hao, S. Li, J. Li, C. Meng, Denitrification of simulated municipal wastewater treatment plant effluent using a three-dimensional biofilm-electrode reactor: operating performance and bacterial community, Bioresour. Technol. 143 (2013) 178–186.
[7] S. Zhang, H.L. Song, X.L. Yang, K.Y. Yang, X.Y. Wang, Effect of electrical stimulation on the fate of sulfamethoxazole and tetracycline with their corresponding resistance genes in three-dimensional biofilm-electrode reactors, Chemosphere 164 (2016) 113–119.
[8] M.H. Zhou, W.J. Fu, H.Y. Gu, L.C. Lei, Nitrate removal from groundwater by a novel three-dimensional electrode biofilm reactor, Electrochim. Acta 52 (2007) 6052–6059.
[9] R.X. Hao, C.C. Meng, J.B. Li, An integrated process of three-dimensional biofilm-electrode with sulfur autotrophic denitrification (3DBER-SAD) for wastewater reclamation, Appl. Microbiol. Biotechnol. 100 (2016) 7339–7348.
[10] N.K. Pazarlioglu, A. Telefoncu, Biodegradation of phenol by Pseudomonas putida immobilized on activated pumice particles, Process Biochem. 40 (2005) 1807–1814.
[11] P. She, S. Bo, X.H. Xing, M. van Loosdrecht, Z. Liu, Electrolytic stimulation of bacteria Enterobacter dissolvens by a direct current, Biochem. Eng. J. 28 (2006) 23–29.
[12] X.G. Li, T. Wang, J.S. Sun, X. Huang, X.S. Kong, Biodegradation of high concentration phenol containing heavy metal ions by functional biofilm in bio-electro-reactor, J. Environ. Sci. 18 (2006) 639–643.
[13] N. Velasco-Alvarez, I. Gonzalez, P. Damian-Matsumura, M. Gutierrez-Rojas, Enhanced hexadecane degradation and low biomass production by Aspergillus Niger exposed to an electric current in a model system, Bioresour. Technol. 102 (2011) 1509–1515.
[14] J. Tang, J. Guo, F. Fang, Y. Chen, L. Lei, L. Yang, Oxidation behavior of ammonium in a 3-dimensional biofilm-electrode reactor, J. Environ. Sci. 25 (2013) 2403–2409.
[15] Z. Cheng, X. Hu, Performance and degradation mechanism of a sequencing batch biofilm reactor combined with an electrochemical process for the removal of low concentrations of cefuroxime, Chem. Eng. J. 320 (2017) 93–103.
[16] S.E. Keithley, M.J. Kirisits, An improved protocol for extracting extracellular polymeric substances from granular filter media, Water Res. 129 (2018) 419–427.
[17] F. Zhang, J.H. Yang, K. Dai, Y. Chen, Q.R. Li, F.M. Gao, R.J. Zeng, Characterization of microbial compositions in a thermophilic chemostat of mixed culture fermentation, Appl. Microbiol. Biotechnol. 100 (2016) 1511–1521.
[18] D. Zheng, Q.B. Chang, Z.W. Li, M.C. Gao, Z.L. She, X.J. Wang, L. Guo, Y.G. Zhao, C.J. Jin, F. Gao, Performance and microbial community of a sequencing batch biofilm reactor treating synthetic mariculture wastewater under long-term exposure to norfloxacin, Bioresour. Technol. 222 (2016) 139–147.
[19] Z.H. Diao, J.J. Liu, Y.X. Hu, L.J. Kong, D. Jiang, X.R. Xu, Comparative study of Rhodamine B degradation by the systems pyrite/$H_2O_2$ and pyrite/persulfate: reactivity, stability, products and mechanism, Separ. Purif. Technol. 184 (2017) 374–383.
[20] N. Ailijiang, J.L. Chang, P. Liang, P. Li, Q. Wu, X.Y. Zhang, X. Huang, Electrical stimulation on biodegradation of phenol and responses of microbial communities in conductive carriers supported biofilms of the bioelectrochemical reactor, Bioresour. Technol. 201 (2016) 1–7.
[21] A.N. Alshawabkeh, Y.P. Shen, K.Y. Maillacheruvu, Effect of DC electric fields on COD in aerobic mixed sludge processes, Environ. Eng. Sci. 21 (2004) 321–329.
[22] Y. Feng, X. Li, T. Song, Y.Z. Yu, J.Y. Qi, Stimulation effect of electric current density (ECD) on microbial community of a three dimensional particle electrode coupled with biological aerated filter reactor (TDE-BAF), Bioresour. Technol. 243 (2017) 667–675.
[23] V. Sanchez-Vazquez, I. Gonzalez, M. Gutierrez-Rojas, Electric field as pretreatment to enhance the activity of a whole-cell biocatalyst for hydrocarbon degradation in contaminated water, Chem. Eng. J. 260 (2015) 37–42.
[24] V.I. Podolska, V.N. Ermakov, L.N. Yakubenko, Z.R. Ulberg, N.I. Gryshchenko, Effect of low-intensity pulsed electric fields on the respiratory activity and electrosurface properties of bacteria, Food Biophys. 4 (2009) 281–290.
[25] G. Lustrato, G. Alfano, C. Belli, L. Grazia, M. Iorizzo, G. Ranalli, Scaling-up in industrial winemaking using low electric current as an alternative to sulfur dioxide addition, J. Appl. Microbiol. 101 (2006) 682–690.
[26] P. Arulazhagan, C. Sivaraman, S.A. Kumar, M. Aslam, J.R. Banu, Co-metabolic degradation of benzo(e)pyrene by halophilic bacterial consortium at different saline conditions, J. Environ. Biol. 35 (2014) 445–452.
[27] R.A. Kanaly, S. Harayama, K. Watanabe, Rhodanobacter sp strain BPC1 in a benzo[a]pyrene-mineralizing bacterial consortium, Appl. Environ. Microbiol. 68 (2002) 5826–5833.
[28] S. Rasalingam, R. Peng, R.T. Koodali, An insight into the adsorption and photocatalytic degradation of rhodamine B in periodic mesoporous materials, Appl. Catal. B Environ. 174 (2015) 49–59.
[29] D.P. Kelly, Y. Uchino, H. Huber, R. Amils, A.P. Wood, Reassessment of the phylogenetic relationships of Thiomonas cuprina, Int. J. Syst. Evol. Microbiol. 57 (2007) 2720–2724.
[30] F. Battaglia-Brunet, C. Joulian, F. Garrido, M.C. Dictor, D. Morin, K. Coupland, D.B. Johnson, K.B. Hallberg, P. Baranger, Oxidation of arsenite by Thiomonas strains and characterization of Thiomonas arsenivorans sp nov, Anton. Leeuw. Int. J. G. 89 (2006) 99–108.
[31] S. Szekeres, I. Kiss, M. Kalman, M. Ines, M. Soares, Microbial population in a hydrogen-dependent denitrification reactor, Water Res. 36 (2002) 4088–4094.
[32] K.J. Chin, P.H. Janssen, Propionate formation by Opitutus terrae in pure culture and in mixed culture with a hydrogenotrophic methanogen and implications for carbon fluxes in anoxic rice paddy soil, Appl. Environ. Microbiol. 68 (2002) 2089–2092.
[33] C. Zhang, Y.H. Jiang, Y.L. Li, Z.X. Hu, L. Zhou, M.H. Zhou, Three-dimensional electrochemical process for wastewater treatment: a general review, Chem. Eng. J. 228 (2013) 455–467.
[34] H.S. Lee, K. Lee, Bioremediation of diesel-contaminated soil by bacterial cells transported by electrokinetics, J. Microbiol. Biotechnol. 11 (2001) 1038–1045.